Tectonophysics 566-567 (2012) 95–104

Contents lists available at SciVerse ScienceDirect

Tectonophysics

journal homepage: www.elsevier.com/locate/tecto

Fluid-triggered earthquake swarms in the Rwenzori region, East African Rift—Evidence for rift initiation

Michael Lindenfeld [a,*], Georg Rümpker [a], Klemens Link [b], Daniel Koehn [c], Arthur Batte [a,d]

[a] Institute of Geosciences, Goethe University Frankfurt, Altenhöferallee 1, 60438 Frankfurt am Main, Germany
[b] Institute of Geosciences, University of Mainz, Becherweg 21, 55099 Mainz, Germany
[c] School of Geographical & Earth Sciences, University of Glasgow, Scotland, UK
[d] Department of Geology, Makerere University Kampala, Uganda

ARTICLE INFO

Article history:
Received 6 January 2012
Received in revised form 5 July 2012
Accepted 11 July 2012
Available online 28 July 2012

Keywords:
East African Rift
Seismicity
Earthquake swarms
Magmatic intrusions
CO2 degassing
Melt

ABSTRACT

The Rwenzori Mountains are located within the Albertine Rift Valley in western Uganda. To monitor the microseismic activity in the area we have deployed a seismic network of up to 35 stations for a period of about 20 months. The analysis of the recordings revealed several earthquake clusters within a restricted area NE of the mountain block. The clusters form elongated pipes with 1–2 km diameter and vertical extensions of 3–5 km. Most of them are located in 5–16 km depths; however one cluster reaches down to 22 km. Each cluster is composed of a series of single earthquake swarms with durations between a few days and more than a week, interrupted by intervals of inactivity of up to several months. Some of the swarm events exhibit vertical migration tendencies with estimated velocities between 0.3 and 1 km/day. Local magnitudes range from $M_L = 0.5$ to $M_L = 4.0$ with b-values between 0.96 and 1.2. The source mechanisms of the swarm earthquakes are dominated by normal faulting with tension-axes orientations perpendicular to the rift axis. There are only few strike-slip events and no reverse mechanisms. From petrological considerations we presume that the earthquake swarms are triggered by fluids and gases which originate from a magmatic source below the crust. Melt and/or CO_2 are guided along the intersection lines of two steep fault sets that were identified by shear-wave splitting analysis and fault mapping in the Rwenzori area. The existence of a magmatic source within the lithosphere is supported by the detection of a shear-wave velocity reduction in 55–80 km depth from receiver-function analysis and the location of mantle earthquakes at about 60 km. We interpret these observations as indication for an initial rifting process that may eventually lead to the complete detachment of the Rwenzori block from the surrounding rift flanks.

1. Introduction

Earthquake swarms are defined as episodic series of seismic events that are clustered in space and time (Mogi, 1963). Unlike a typical mainshock–aftershock sequence, where the aftershocks have significant lower magnitudes than the mainshock, the earthquake swarms are characterized by a gradual increase and decrease of activity with no predominant primary earthquake. They are commonly associated with magmatic intrusions and fluid transport in the crust reducing the resistance of faults, as well as with stress perturbations induced by the release of volatiles like CO_2 (e.g. Bräuer et al., 2003; Dahm et al., 2008; Hainzl, 2004; Hainzl and Ogata, 2005). The majority of them are observed in regions of active volcanism (Benoit and McNutt, 1996; Gardine et al., 2011; Karpin and Thurber, 1987). Volcanic earthquake swarms are characterized by large b-values between 1.0 and 2.5 which are commonly attributed to a highly fractured crust and a heterogeneous stress field in these areas (Bridges and Gao, 2006; Mogi, 1963). Numerous earthquake swarms are reported from Iceland. Most of them are discussed in the context of magma movements and dike intrusions accompanying volcanic eruptions (Hensch et al., 2008; Jakobsdóttir et al., 2008; Key et al., 2011; Soosalu et al., 2010; White et al., 2011). In many cases the swarm events exhibit a systematic hypocentre migration reflecting the magma intrusion process. Earthquake swarms were also recorded in several sections of the East African Rift, such as Afar, Ethiopian Rift (e.g. Ebinger et al., 2008; Keir et al., 2011), the southern Kenya rift (Ibs-von Seht et al., 2001; Tongue et al., 1994; Young et al., 1991), and the north Tanzanian divergence (Albaric et al., 2010; Baer et al., 2008). In general, these events are attributed to magmatic dike intrusions. However, although the western branch of the East African Rift reveals significant higher seismic activity than the eastern branch, there have been no observations of earthquake swarms in this part of the EARS so far.

Apart from volcanic areas, earthquake swarms are also observed in intraplate regions such as the Bohemian Massive, the French Massive

* Corresponding author.
E-mail addresses: lindenfeld@geophysik.uni-frankfurt.de (M. Lindenfeld), rumpker@geophysik.uni-frankfurt.de (G. Rümpker), linkk@uni-mainz.de (K. Link), daniel.koehn@glasgow.ac.uk (D. Koehn), batte@geophysik.uni-frankfurt.de (A. Batte).

0040-1951/$ – see front matter © 2012 Elsevier B.V. All rights reserved.
http://dx.doi.org/10.1016/j.tecto.2012.07.010

Central, Central Italy, and Long Valley, California. Špičák (2000) gives a compilation of intraplate and artificially induced earthquake swarms. The author finds similar swarm patterns and concludes that the cause is related to intrusion of fluids. The western Bohemia/Vogtland area is one of the most prominent earthquake swarm regions, situated within the Eger rift which is part of the European rift system. Here, earthquake swarms have been reported since the 16th century (Grünthal, 1989). Many investigations manifest that fluids and the transport of mantle volatiles originating from a subcrustal magma body might be the source of the observed swarm activity in this area (Bräuer et al., 2003; Geissler et al., 2005; Špičák and Horálek, 2001; Špičák et al., 1999; Weise et al., 2001).

Ibs-von Seht et al. (2008) analyse earthquake swarms in selected continental rifts. They compare the characteristics of clusters observed in the Rio Grande rift, North America, the Eger rift, Europe, and the Kenya rift, East Africa. They conclude that all investigated swarms occur in rift sections that are influenced by intersecting fracture zones. During the swarm activity the maximum observed magnitudes range from 4.2 to 4.7 and the b-values for all three areas are between 0.8 and 1.0. This corresponds to the magnitude distribution of regular tectonic earthquakes and indicates a difference to earthquake swarms in regions of active volcanism that show b-values significantly higher than 1. There is no clear terminological discrimination between earthquake "swarms" and "clusters". In general, clusters are a series of earthquakes spatially-concentrated with regular patterns, whereas seismic swarms are concentrated in space and occur within a relatively short period of time. In this paper we use the word "cluster" if we refer only to the spatial distribution of a group of earthquakes. In case we discuss the temporal characteristics we prefer the term "swarm".

We focus on the observation of earthquake clusters that were detected during a microseismic monitoring campaign in the Rwenzori region of the East African Rift System (EARS) from February 2006 to September 2007. We describe the characteristics, similarities, and differences to earthquake swarms in other regions. Finally we discuss possible mechanisms for the triggering of the swarm events with respect to petrological information from the region.

2. Tectonics and seismicity of the Rwenzori region

The ~3000 km long Cainozoic EARS extends from the Afar triple junction in the north to Mozambique in the south. In southern Ethiopia it splits up into two branches surrounding Lake Victoria: The eastern branch passes Kenya and terminates in northern Tanzania, the western branch runs through Lake Albert, Lake Edward, Lake Tanganyika, and Lake Malawi, and ends in southern Mozambique. The 5000 m high Rwenzori Mountains are situated within the Albertine rift, which is part of the western branch of the EARS (Fig. 1). They represent a non-volcanic basement block composed of rocks of Proterozoic and Achaean age (Link et al., 2010) whose origin and relation to the evolution of the EARS are focus of the RiftLink project (www.riftlink.org). The Rwenzoris are bounded by two rift segments: (a) the Albertine rift, extending west of the mountains from Lake Edward in the south to Lake Albert in the north, and (b) the Lake George rift segment running east of the mountains starting at Lake Edward and ending up north of Lake George at about 0.5°N latitude. Previous studies indicate that the Lake Albert rift started in the north and propagated southwards whereas the Lake Edward–George segment started in the Lake Edward region and propagated northwards (Koehn et al., 2008; Morley, 1999). Such propagation may lead to a clockwise rotation of the Rwenzori block (Koehn et al., 2008), which in turn can lead to complex intersecting faults in the NE of the Rwenzori (Koehn et al., 2010), where the Rwenzori may break off the Victoria plate. The area of focus is cluttered with quaternary volcanic craters. Four volcanic fields mark the centres of magmatic activity (Fig. 1); these are the Katwe-Kikorongo and Bunyaruguru fields in the south and south-east, the Ndale field in the east and the Fort Portal field in the north-east of the Rwenzori

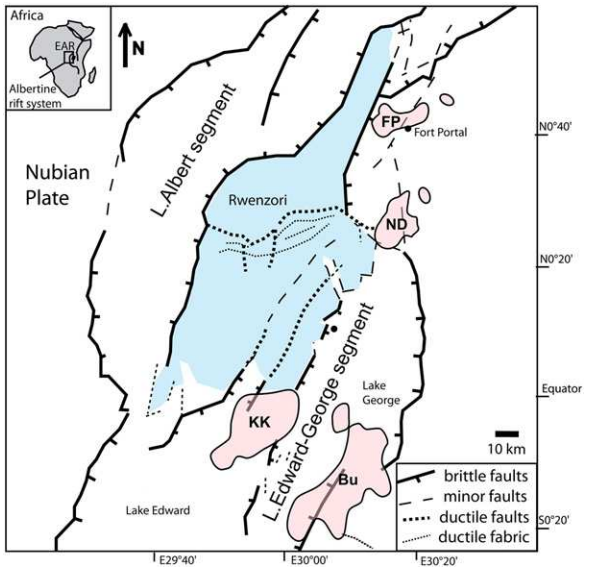

Fig. 1. Tectonic map of the Rwenzori area (after Koehn et al., 2008, 2010). The Rwenzori mountains (light blue area) are surrounded by two rift segments, with the exception of a region in the NE, where they are connected to the Victoria plate. Volcanic fields are marked by red areas (FP: Fort Portal, ND: Ndale, KK: Katwe-Kikorongo, Bu: Bunyaruguru).

Mountains. The southern fields are separated and affected by the rift while the northern fields are located on the unrifted Precambrian bridge that connects the Rwenzori Mountain chain with the flanks. The time of volcanic activity ranges from 50 ka in the south (Boven et al., 1998) to Holocene (8–4 ka) in the Katwe-Kikorongo and the northern fields (Barker and Nixon, 1989; Brooks and Smith, 1987).

From global observations it is known that the western branch of the EARS shows significant higher seismic activity than the eastern branch, with the Rwenzori region being the area with highest seismicity of the entire rift system (e.g. Albaric et al., 2009; Fairhead and Girdler, 1971; Foster and Jackson, 1998; Nyblade and Langston, 1995; Twesigomwe, 1997). Previous microearthquake surveys in the Rwenzori region by Maasha (1975), Tugume and Nyblade (2009), and Lindenfeld et al. (2012) confirm the high seismicity rate.

The results of Lindenfeld et al. (2012) are based on a seismometer network covering an area of roughly 80 km × 140 km and operating from February 2006 to September 2007 (Fig. 2). The recordings reveal high seismic activity with approximately 800 events per month. The majority of located events lie within faults zones to the east and west of the Rwenzoris with the highest seismic activity observed in the north-eastern area, where the mountains are in contact with the rift shoulders. Local magnitudes range from $M_L = -0.5$ up to $M_L = 5.1$ with a b-value of 1.1. In the northern part of the network with its high station density the earthquake catalogue is complete for magnitudes larger than 0.8.

The hypocentral depth distribution exhibits a pronounced peak of seismic energy release at 15 km. The maximum depth extent varies between 20 km and 32 km and correlates well with Moho depths that were derived from P-wave receiver functions by Wölbern et al. (2010). Vertical profiles indicate that beneath the rift shoulders seismicity extends from the surface down to approximately 30 km depth, whereas beneath the rift valley seismicity is restricted to depths between 10 km and 20 km. However, Lindenfeld and Rümpker (2011) report the detection of a group of mantle earthquakes in this area probably associated with magmatic processes in the lithospheric mantle, (see Fig. S1 in the supplementary information for details).

Fault plane solutions of 304 events were derived from P-wave polarities and S/P amplitude ratios. The majority of the source mechanisms exhibit pure or predominantly normal faulting with highly

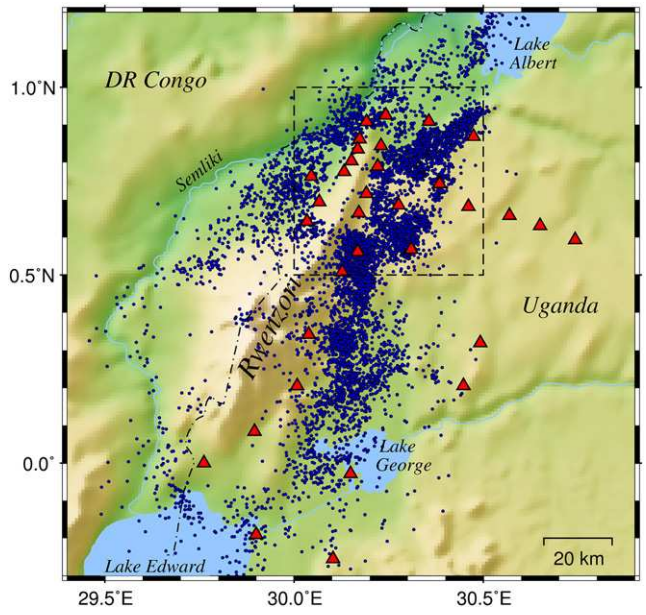

Fig. 2. Seismic station network (triangles) and recorded local seismicity from February 2006 to September 2007 (from Lindenfeld et al., 2012). The dashed frame indicates the central area map presented in Fig. 3.

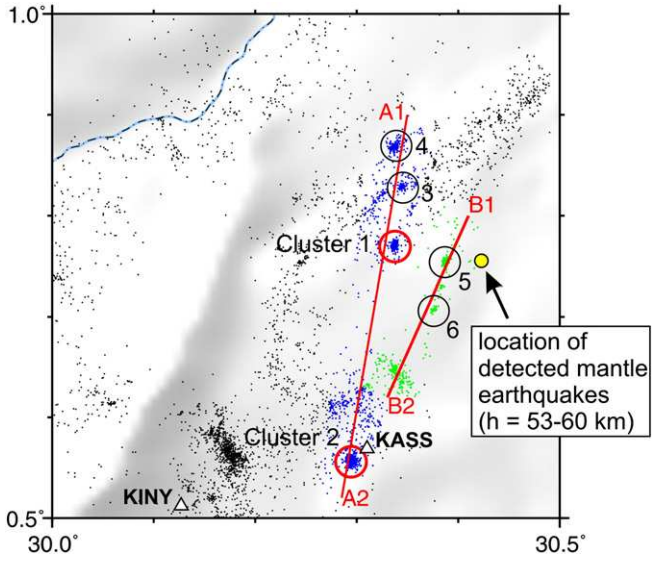

Fig. 3. The central region for which earthquakes are relocated by the HypoDD method (dashed rectangle in Fig. 2). Two profiles (A1-A2 and B1-B2) indicate the positions of the vertical sections presented in Fig. 4a and b. Coloured symbols (blue, green) mark epicentres that are projected onto the respective profile line. The yellow dot marks the location of the mantle earthquakes (Lindenfeld and Rümpker, 2011). The swarm activity of two clusters (cluster 1 and 2, red circles) is presented in this paper. Seismograms of two stations (KASS, KINY) are presented in Section 3.4 of this paper.

uniform T-axis trends oriented WSW-ENE, which is in good agreement with kinematic rift models (Lindenfeld et al., 2012; Stamps et al., 2008, 2010).

3. Observation of earthquake swarms

3.1. Hypocentre relocation and identification of earthquake clusters

A closer inspection of the epicentral distribution reveals several earthquake clusters in the north-eastern region of the network. To verify this observation we relocated the data set described in Lindenfeld et al. (2012) by applying the double-difference algorithm (hypoDD) of Waldhauser and Ellsworth (2000) to derive more precise relative locations than those obtained by standard single-event location methods. The hypoDD technique minimizes residual travel time differences of earthquake pairs at a common station by weighted least squares using a singular value decomposition algorithm. If the hypocentral distance between the paired events is small compared to the event-station distance then the travel time residuals are affected only marginally by local velocity variations resulting in more accurate relative hypocentre locations.

Initially more than 10000 events were selected for relative location but due to large event-event spacing and unfavourable station configuration the hypoDD algorithm rejected about 25% of the data set, especially in the south-western area, where none of the initial hypocentres were relocated. Fig. 3 presents the relocated epicentre distribution within a zoomed area that is characterized by the highest seismicity of the Rwenzori region (dashed box in Fig. 2). The improved location accuracy leads to sharper structural details and reveals several earthquake clusters with almost circular shapes. We were not able to identify further earthquake clusters outside of the map in Fig. 3. The occurrence of earthquake swarms seems to be restricted to the area north-east of the Rwenzoris, where the mountains are connected to the eastern rift shoulder. Furthermore, this zone coincides with the location of the mantle earthquakes in 53–60 km depth (Lindenfeld and Rümpker, 2011). The position of this cluster is marked with a yellow symbol in Fig. 3. Two red profile-lines indicate the position of vertical sections each of them transecting several earthquake clusters.

3.2. Cluster depth distribution

The hypocentral depth distribution along profiles A1-A2 and B1-B2 is plotted in Fig. 4a and b, respectively. The vertical section A1-A2 reveals four earthquake clusters which can be clearly separated from the background activity. They are located at depths between 5–16 km with a pronounced pipe-like shape and a vertical extent of 3 km to 5 km. The diameters range from 1–2 km. Two of the clusters (marked as clusters 1 and 2) show a clear hypocentral upward migration and are discussed in Sections 3.3 to 3.6. Details for clusters 3 and 4 are provided in the supplementary information.

Profile B1-B2 is located at the eastern boundary of the seismic active region. The hypocentral depths of the three clusters on this profile (Fig. 4b) show a systematic upward shift beginning at 22 km depth at the northern end of the profile (B1) and reaching approximately 13 km depth at its southern end (B2). The vertical extent of the two deepest clusters (5 and 6) is only 2–3 km (see the supplementary information for details). We note that the detected cluster of mantle earthquakes is located just beneath the lowermost crustal cluster at a depth between 53 km and 60 km.

3.3. Temporal evolution of the earthquake clusters

To show the spatio-temporal characteristics of the earthquake clusters we have plotted the three-dimensional hypocentral distributions of clusters 1 and 2 (Fig. 5). The source times of individual events are coded by different symbol colours. The clusters are characterized by episodic earthquake swarms rather than permanent seismic energy release. The initial phase of cluster 1 (Fig. 5, left) starts with an earthquake swarm in July 2006 covering the entire vertical extent of the cluster between 10 km and 15 km depth and ends in August 2006 (dark blue symbols). After eight months of quiescence the swarm activity resumes in March 2007 (yellow symbols) at the lowermost parts of the cluster (13–12 km depth). Subsequent swarm events show a systematic upward migration to a depth of about 10 km (orange and red symbols). The swarm activity of cluster 1 ends in July 2007. Cluster 2 (Fig. 5, right) is active between December

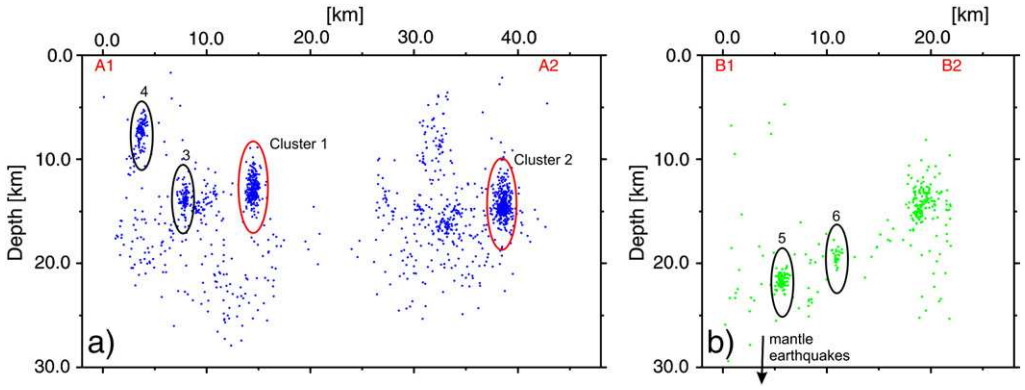

Fig. 4. Vertical sections along profiles (a) A1-A2 and (b) B1-B2 (see Fig. 3). The two event clusters (marked by red ellipses) are discussed in detail in Sections 3.3 to 3.6. The position of the mantle earthquakes located at 53–60 km depth (Lindenfeld and Rümpker, 2011) is indicated by an arrow on profile B1-B2.

2006 and July 2007. It shows a similar but less distinct migration tendency compared to cluster 1: Early events (blue colours) are concentrated at about 15–16 km depth. Subsequent events (orange–red) are located at about 12–13 km depth.

Fig. 6 shows the hypocentral depth versus occurrence time for events of cluster 1. The complete cluster consists of 262 earthquakes and is composed of several episodic swarms with durations between a few days up to more than two weeks. The individual swarms are separated by time intervals of quiescence which lasts up to several months. The 4 largest swarm events occurred during 1–22 August 2006, 18–23 April 2007, 21–28 May 2007, and 29 June–1 July 2007, with 71, 27, 54, and 26 events, respectively. The initial phases of three swarm periods are shown in the subfigures. We observe an increase of the vertical cluster extend with time, whereas the basis of the swarm activity is fixed at 13–14 km depth. The dashed lines indicate velocities between 0.3 km/day and 1 km/day of the upward migration. The symbol sizes are proportional to the event magnitudes and indicate that there is no dominant single event in the individual sub-clusters, an observation which is characteristic for earthquake swarms (e.g. Ibs-von Seht et al., 2008).

The spatio-temporal behaviour of cluster 2 is presented in Fig. 12. The whole cluster consists of 451 earthquakes and is built-up of at least 7 swarm bursts, most of them with durations of 1–2 days which are short compared to the swarm durations in cluster 1. The intensity of the single swarm activities seems to increase systematically during the observation period and ends with a huge earthquake swarm lasting from 21 June to 11 July 2007 which consists of 160 events. The upper dashed line indicates a possible migration of the uppermost seismic activity within each swarm, however, the slope of this line is constrained only by few events. As for the case in cluster 1, the lower bound of the seismic activity is located at a fixed depth, here between 16 km and 17 km. After the crisis in June/July 2007 the swarm activity decreases significantly and the vertical extent reduces to the situation at the beginning of the whole cluster in November 2006.

Depth vs. time plots for clusters 3–6 are provided in the supplementary information (Fig. S2). Here, we give a short description of the main characteristics. Cluster 3 consists of a single earthquake swarm of 72 events from 13–20 August 2006. Magnitudes range from $M_L = 0.2$ to $M_L = 1.8$ which is relatively small compared to the

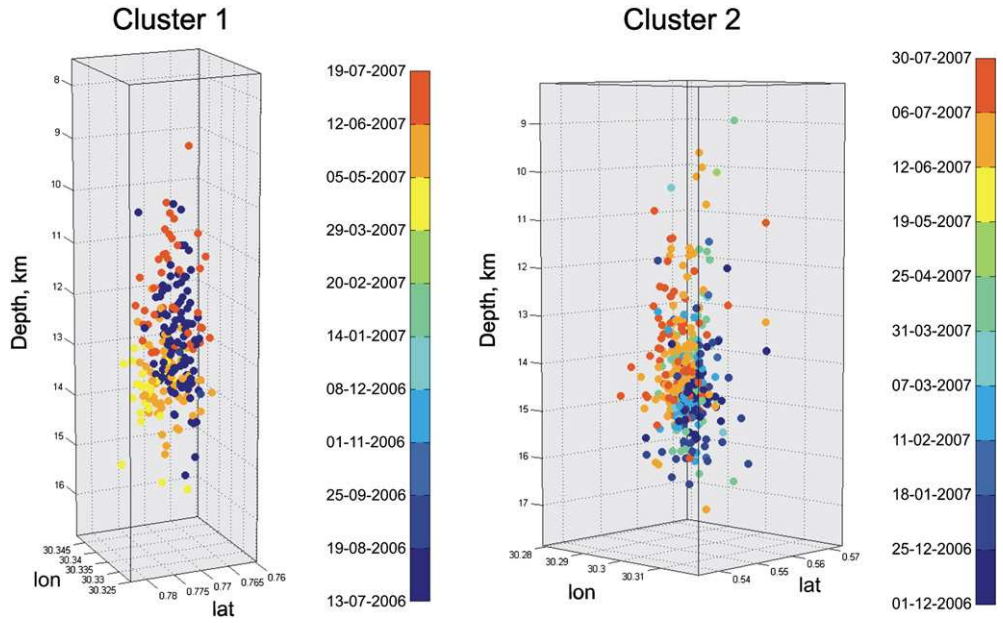

Fig. 5. Three-dimensional hypocentre distribution of clusters 1 and 2. Colours indicate the temporal evolution of the earthquake swarms from July 2006 to July 2007 and from December 2006 to July 2007, respectively. Note that horizontal axes are longitude and latitude in degree; vertical and horizontal dimensions are to scale.

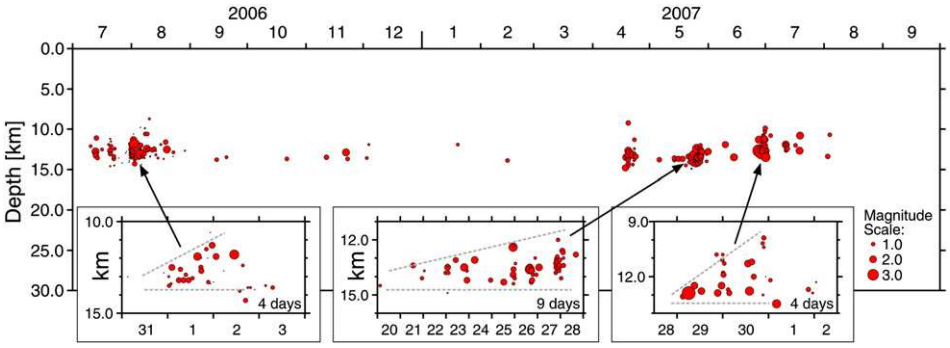

Fig. 6. Hypocentral depth versus source time of events belonging to cluster 1. The symbol size is proportional to magnitude (see legend). The three insets show the initial phase of different earthquake swarms within the cluster. Numbers on the time axes are days of the respective month. Dashed lines indicate a possible upward migration of seismic activity.

other analysed earthquake clusters (up to $M_L = 4.0$). The swarm activity in cluster 4 develops similar as in cluster 2, with increasing intensity and a final maximum earthquake swarm in May 2007. The vertical extent of the swarms ranges between 5 km and 10 km depth, however, the upper and lower bounds of the seismic activity are not well defined. There is no vertical migration visible. Clusters 5 and 6 are located at profile B1-B2. With a vertical extension of 1–2 km and a horizontal diameter of about 1 km they represent rather point sources rather than vertically oriented, elongated pipes. The clusters are located in 22 km and 19 km depth, respectively. In contrast to clusters 1–4 we observe a permanent seismic energy release during the observation period from 2006 to 2007 in a fixed depth, rather than single swarm events.

3.4. Waveform similarity

It is a common feature of earthquake swarms that waveforms of individual events exhibit significant similarity at the recording stations (e.g. Hayashi and Morita, 2003). This occurs mainly because the locations of swarm events are concentrated in a small area and are close to each other. For this reason the ray paths and site responses may be considered identical for these events. Furthermore, the source mechanisms of swarm events are also similar in most cases (e.g. Ibs-von Seht et al., 2008). An example of similar waveforms is given in Fig. 7. The graph shows P-wave signals of two earthquakes belonging to cluster 2 and recorded at two different locations. Station KASS is located close to the cluster centroid with an epicentral distance of 1.9 km, whereas station KINY has a distances of 19.7 km (cf. Fig. 3). There is a substantial waveform similarity at each station which allows to identify common amplitude wiggles in the P-wave group of the events. However, there are significant differences between the two stations. P-waves at KINY are depleted of high frequencies compared to the recordings at KASS. This effect is probably attributed to increasing absorption of seismic energy for longer ray paths. The observed waveform similarities provide an additional indication for a common source mechanism within a certain cluster. More examples of waveform similarity can be found in the supplemental information (Fig. S3).

3.5. Magnitudes

Fig. 8 presents the magnitude–frequency distribution of all swarm events contained in clusters 1–4 (circles). There are 911 events in total with magnitudes between $M_L = 0.1$ and $M_L = 4.0$. This magnitude interval is also observed in swarms of other continental rifts (Ibs-von Seht et al., 2008). Moreover, the cumulative magnitude distribution seems to be characterized by two different slopes (b-values): a relatively small slope between $M_L = 0.8$ and $M_L = 1.8$, and a larger one for $M_L > 1.8$. Such bimodal magnitude–frequency distributions are typical for volcanic areas and indicative for fluid-induced swarm activity (Wiemer and Wyss, 2002). However, a closer inspection of the data revealed that the apparent bimodal distribution is an artefact of different detection thresholds: During night-time (21:00–7:00 local time) the seismometer network has its highest sensitivity with a magnitude of completeness $M_C \approx 0.8$. During day-time (7:00–21:00 local time) the sensitivity is considerably reduced by human activity, such as field work and traffic. The increased noise level at that time reduces the number of located small events and increases the magnitude of completeness to $M_C \approx 1.8$. Therefore, the cumulative magnitude–frequency distribution of the combined day and night events will exhibit two discontinuities at $M_{C1} = 0.8$ and $M_{C2} = 1.8$, respectively, which could be interpreted erroneously as a bimodal distribution with two b-values. The magnitude distribution of the night events alone (triangles in Fig. 8) is characterized by a unique magnitude of completeness at $M_C = 0.8$ and a single b-value of 1.0 (calculated by a linear least squares fit). These values are similar

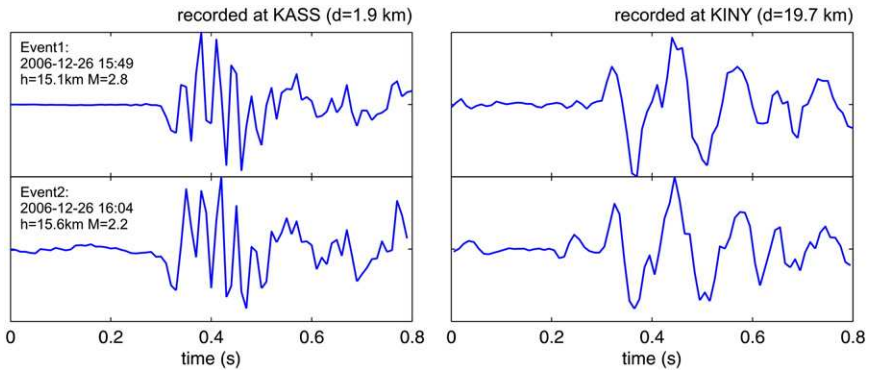

Fig. 7. Waveform similarity of cluster events. The plot shows the P-waves of two events (upper and lower rows) belonging to cluster 2 and recorded at stations KASS (left column) and KINY (right column) (see Fig. 3 for position of cluster and stations). Labels d, h, and M indicate epicentral distance, hypocentral depth, and local magnitude, respectively.

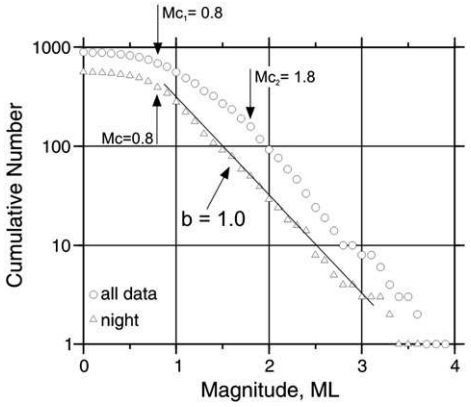

Fig. 8. Magnitude frequency distribution of swarm events in clusters 1–4. Circles: all events. The distribution includes two magnitudes of completeness: $M_{C1}=0.8$ for night-time events and $M_{C2}=1.8$ for day-time events caused by different noise levels during the respective periods. The shape of the graph is biased by the different characteristics of day-time and night-time events and should not be interpreted as bimodal with two different b-values. Triangles: magnitude distribution for the night-time events of clusters 1–4. This homogeneous subset of data has a b-value of 1.0.

to the b-values derived for the whole earthquake catalogue of the Rwenzori region (b = 1.1, Lindenfeld et al., 2012), but slightly higher than in other continental earthquake swarms (b = 0.8). According to Mogi (1963) b-values between 0.5 and 1.0 are indicative of tectonic processes in non-volcanic intraplate areas. Larger b-values (1.0–2.5) are usually observed in regions with active volcanism, where seismicity is associated with eruptions and magma movements (e.g. Karpin and Thurber, 1987). Our observation (b = 1.0) is located just in between and does not allow to discriminate between pure tectonic and magmatic processes.

3.6. Source mechanisms

Source mechanisms of 55 events in cluster 2 were derived from P-wave polarities and S/P amplitude ratios using a grid search algorithm to determine the orientation of the nodal planes (FOCMEC by Snoke et al., 1984). A compilation of the individual mechanisms is given in the supplementary information (Fig. S4). As a synopsis Fig. 9 presents a classification of the derived fault plane solutions on the basis of P- and T-axis plunge angles. The majority of mechanisms are normal faulting (red symbols) or predominantly normal faulting

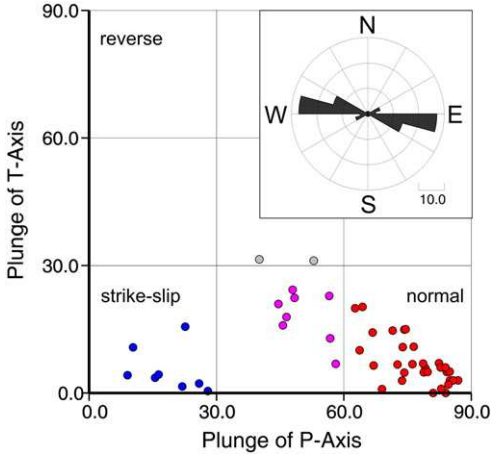

Fig. 9. Classification of the source mechanisms of cluster 2 according to the plunge angles of the P- and T-axes. Normal faulting (red symbols) predominates - with a few strike-slip mechanisms (blue symbols). There is no reverse faulting in the earthquake swarm. The rose diagram in the upper right corner indicates the T-axes trends of the derived fault-plane solutions.

(pink symbols) with a minor group of strike-slip events (blue symbols). None of the analysed swarm events can be associated to reverse faulting. This is different to the distribution of source mechanisms in the whole Rwenzori region, for which we observed also reverse faulting mechanisms (Lindenfeld et al., 2012). The directions of the tension axes (T-axis trends) are plotted in a rose-histogram (Fig. 9, upper right). The results reveal a considerable uniform picture for the extensional stress field which is oriented WNW-ESE, perpendicular to the rift axis. This is in agreement with kinematic rift models (Stamps et al., 2008, 2010) and indicates that the source mechanisms of the swarm events are controlled by the regional stress field associated with the extensional regime.

4. Discussion

4.1. General features of the observed earthquake swarms

The earthquake swarms of the Rwenzori area show numerous similarities in comparison with earthquake swarms observed in other continental rifts (see Ibs-von Seht et al., 2008, for a compilation of properties): Clusters 1, 2, 3, and 4 on profile A1-A2 are located in the crust at depths between 5 km (or less) and 16 km. The duration of individual swarms within each cluster is spread between a few days up to months. Only in cluster 1 we observe a clear upward migration of seismic activity. The remaining clusters exhibit weak or no vertical migration. This variation corresponds to reports from other regions which range from “clear migration” (Kenya rift), “diffuse migration” (Eger rift) to “no migration” (Rio Grande rift). Magnitudes of the analysed clusters reach maximum values of $M_L=4.0$ with a b-value of 1. This agrees well with the compilation of Ibs-von Seht et al. (2008) which states maximum $M_L=4.7$ and b = slightly less or close to 1. There is no single predominating event within an earthquake swarm. Fault plane solutions indicate an extensional or strike-slip stress regime, no reverse faulting is observed. The orientation of the source mechanisms is controlled by the regional stress field. Recorded waveforms of different cluster events are almost identical at individual stations.

4.2. Cluster location and shape

All of the identified earthquake clusters in the Rwenzori region are located within a restricted area north-east of the mountains (Fig. 3). The question arises whether this observation is possibly an artefact due to the heterogeneous station distribution. To the north of Lake George, between 0.1° and 0.4° latitude, the inter-station distances increase significantly which leads to an increased event detection threshold. In this region the earthquake catalogue is complete for magnitudes larger than $M_L=1.2$ (compared to $M_L=0.8$ in the cluster area) which prevents the detection of small earthquakes that build up the majority of an earthquake swarm. For this reason it might be impossible to detect earthquake clusters outside of the area of high station density.

To verify this assumption we compared the complete earthquake catalogue with the data set containing only events with $M_L>1.2$, simulating a quasi-homogenous earthquake catalogue with constant detection threshold over the whole region (Fig. S5, supplements). Although a significant number of small earthquakes are now omitted in the epicentre map, we are still able to identify the already established event clusters because they contain a sufficient number of stronger events. This implies that earthquake clusters in other parts of the region should also be detectable, if they are comparable to the identified clusters in terms of magnitude distribution and number of events. Since we do not observe significant earthquake accumulation outside the marked area, we conclude that the major swarm activity is indeed restricted to the observed region. This observation provides further constraints on

their origin and their implication for the rift evolution, as discussed below.

Most earthquake swarms in rifting regimes are related to magmatic dike intrusion or fluid-transport processes in crustal faults. As might be expected these clusters form vertical oriented, planar shapes tracing the outline of the dike or fault, e.g. in Iceland (Jakobsdóttir et al., 2008), in the Eger rift (Dahm et al., 2008), Afar (Ebinger et al., 2008) or the southern Kenya rift (Ibs-von Seht et al., 2001). In contrast, we observe concentrated vertically-oriented pipe-like clusters, which have not been reported previously for the East African rift. Most observations of those earthquake patterns are related to magma transport in conduits beneath active volcanoes, like Piton de la Fournaise, Réunion Island (Battaglia et al., 2005) or Eyjafjallajökull in Iceland (Tarasewicz et al., 2012).

Hensch et al. (2008) report hypocentre migration of earthquake swarms in the Tjörnes Fracture Zone (North Iceland) induced by rising magma dikes. They observe that the swarm activity concentrates above an ascending dike due to stress accumulations at the top tip. This leads to an upward migration of the whole earthquake swarm, including its base. In contrast, we observe swarms with increasing vertical extent, however, in all cases the base is located at a fixed depth. Therefore it is unlikely that these earthquakes are directly induced by ascending magmatic dikes. We rather think that the release of magmatic fluids or gases in certain crustal depths – depending on the environment conditions – could induce the observed swarm activity.

Fluid migration along intersection lines of vertically-oriented fault systems would explain the observed pipe-like cluster patterns. In the NE of the Rwenzoris we find two dominant fault systems (Fig. 10a) that show a very steep intersection lineation. Fault set 1 is oriented parallel to the main rift faults and corresponds to the far field extension direction. Fault set 2 is almost perpendicular to fault set 1 and is only found NE of the Rwenzori, at the northern end of the Lake George rift and along the intersection of the Rwenzori with the rift flank. This fault set is also reported in Koehn et al., 2010 (intersection faults) and may represent a local stress field that develops as the Rwenzori block breaks off from the Victoria plate. The geometry of the Rwenzori block within the rift will lead to a clockwise rotation of the block (Koehn et al., 2008) and this in turn may trigger faults with a NE-SW extension and a NW-SE trend (set 2 faults). The intersection lineation of these two steep fault sets is also steep. Since both fault sets are mainly extensional their intersection will represent vertical pipe-like structures that can act as preferred pathways for fluids, gas or melt.

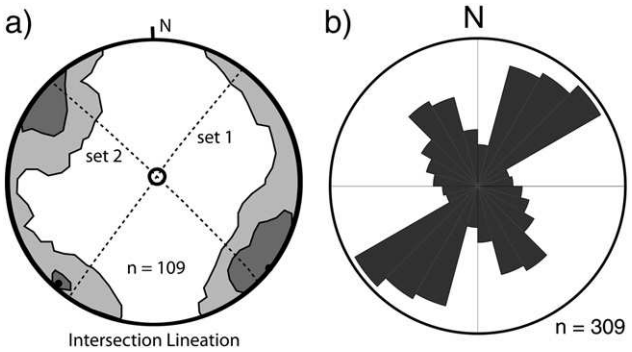

Fig. 10. (a) Lower hemisphere stereonet plot showing the p-pole distribution of faults in the N and NE of the Rwenzoris. Two maxima are indicated by darker shading. Great circles that cross the two maxima are plotted and labelled fault set 1 and fault set 2, respectively. The intersection of these two major fault sets, as indicated by the black circle, corresponds to an almost vertical line. (b) Results of shear wave splitting analysis from local earthquakes in the Rwenzori region. The histogram shows the azimuthal distribution of the fast-polarization directions binned within 15° wide sectors. The bimodal pattern corresponds to two sets of fault systems: The first one strikes in NE direction, parallel to the rift axis, the second one is oriented almost perpendicular to this, in NNW direction.

These observations are complemented and supported by the analysis of shear wave splitting parameters of local earthquakes in the Rwenzori area that were obtained by a cross-correlation method. The orientations of the fast velocity axes exhibit a distinct bimodal distribution (Fig. 10b), almost identical to the fault pattern mapped by Koehn et al. (2010) (Fig. 10a). The majority of the fast axes are aligned in NE–SW direction, parallel to the main rift faults, whereas a significant fraction of the data set has a NNW–SSE trend, almost perpendicular to the rift axis. Seismic anisotropy in the crust is assumed to be caused by stress-induced parallel faults with fast velocity axes oriented parallel to the fault trends (e.g., Crampin and Chastin, 2003). Therefore, the shear wave splitting results may reflect the same two intersecting groups of faults as observed by Koehn et al. (2010).

4.3. Indications for fluid triggered swarm activity

According to petrological indications the earthquake swarms in the Rwenzori area are presumably caused by fluid movements and gas release in the crust originating from a deeper magmatic body. The clusters are situated between two quaternary volcanic fields, the Fort Portal field in the north and the Ndale field to the south of the cluster area (cf. Fig. 1). The water and CO_2-rich lavas are silica undersaturated, strongly alkaline and calcium-rich (Foley et al., 2012). They range from strongly potassic lavas to alkaline melilitite associated with calcic carbonatites (Bailey et al., 2005; Hogarth and Horne, 1989; Stoppa et al., 2000). The majority of the exposed lavas are vesicular and thus indicate free gas phases at low pressures. The deep and very large explosion craters are indicative of explosive, probably volatile and gas rich, volcanic eruptions.

Furthermore, the observed wide spread active thermal, saline and gaseous springs that are rich in sulphate and free CO_2 (Dixon and Morton, 1970), travertines and dry gas vents (pers. comm., Geological survey of Uganda) suggest ongoing subsurface magmatic activity throughout the region. The compositions and isotope ratios of the mineral waters and their incorporated gases also point to a mixing with a magmatic or mantle related gas flow and water source (Arad and Morton, 1969; Bahati et al., 2005; Kato, 2000).

Rosenthal et al. (2009) show that the volcanic fields require an oxidized, hydrated and carbonated source within the mantle below 80 km. Thus it is presumable that the initial primer melt contains H_2O as well as CO_2. Primitive melilitites naturally contain up to 8 wt% CO_2 (Eggler, 1989). But yet at mantle pressure conditions >1 GPa the high CO_2-solubility of 10–20 wt% in alkali rich melt (Brooker et al., 2001) should inhibit carbonatite or CO_2 immiscibility (Brooker and Kjarsgaard, 2011). When the melt ascends to lower pressures the vapour saturation of CO_2 will eventually be reached and CO_2 as a free phase can be released. Regarding alkaline, silica undersaturated melts, these should be below 1 GPa (Brooker and Kjarsgaard, 2011) and above 0.5 GPa (Dixon, 1997) equivalent to approximately above 30 km and below 15 km depth, somewhere in the lower middle crust. As the saturation limit of the melt continuously decreases with decreasing pressure and temperature the degassing will continuously proceed (Newman and Lowenstern, 2002). Depending on the melt composition the degassing continues towards the surface until little $CO_2 \ll 500$ ppm is remaining in the melt (Dixon, 1997). During this process the released gas phases will expand due to the lower ambient pressure with shallower depths and the accompanying stress perturbations can trigger the observed earthquake swarms.

The existence of the postulated magmatic body in the mantle is also supported by the analysis of S-wave receiver functions which provides evidence for two consecutive reductions in shear-wave speed at depths between 55–80 km and 140–160 km, respectively (Wölbern et al., 2012). The deeper discontinuity is interpreted as the lithosphere–asthenosphere boundary, whereas the shallower

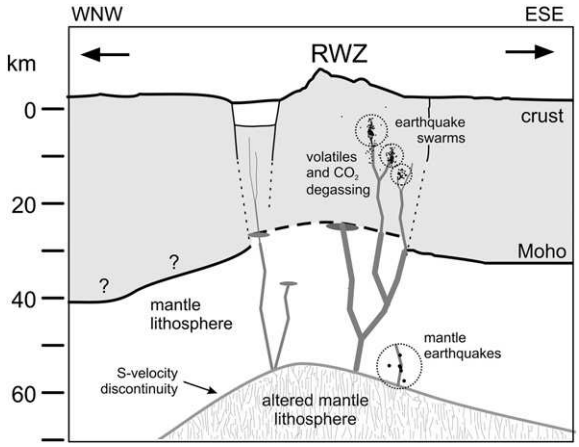

Fig. 11. Cartoon illustrating the system of magma and fluid transport in the lithosphere beneath the Rwenzori region. The locations of mantle earthquakes and earthquake swarms are indicated. The depths of the Moho and of an upper mantle discontinuity are documented by P- and S-wave receiver functions (Wölbern et al., 2010, 2012, Abstract).

discontinuity likely marks the upper bound of an altered mantle lithosphere that might be composed by melt infiltrations. The observation of mantle earthquakes within the same depth range is a further indication of magmatic fracturing and dyke emplacement close to the detected discontinuity. A cartoon (Fig. 11) illustrates the principles of the discussed mechanisms.

The observed earthquake swarms in the Rwenzori region exhibit several similarities with the occurrence of earthquake swarms in the Eger rift. Especially the spatio-temporal properties show considerable correlations. As an example we present a depth vs. time plot of an earthquake swarm recorded in the Eger rift (Fig. 12, top) together with the depth vs. time plot of cluster 2 events (Fig. 12, bottom). In both cases the earthquake cluster consists of a series of single earthquake swarms each lasting from few days up to 1–2 weeks and separated by inactive periods of up to one month duration. They have comparable vertical extensions and similar depths. The occurrence of earthquake swarms in the Eger rift is likewise attributed to transport of fluids ascending along deep reaching fracture system from a magmatic body at the base of the lower crust or in the upper mantle (Bräuer et al., 2003; Geissler et al., 2005; Ibs-von Seht et al., 2008; Weise et al., 2001). The migration of magmatic volatiles coincides with pressure perturbations that are able to trigger earthquakes within the crust (Bräuer et al., 2003). Fluid-injection-experiments at the KTB borehole have shown that even small pressure variations (<1 MPa) triggered numerous microearthquakes at a depth of 9 km (Zoback and Harjes, 1997).

5. Conclusions

The results of our study suggest that the observed earthquake swarms in the Rwenzori area originate from crustal fluid migrations and/or CO_2 emanations rising from a magmatic body in the upper mantle. The model shown in Fig. 11 gives an impression of possible mechanisms that trigger the observed swarm activities. The transport of these volatiles concentrates along vertical oriented intersections of pre-existing crustal fault systems accompanied by pressure perturbations which are able to trigger the observed pipe-shaped earthquake swarms. The occurrence of mantle earthquakes just beneath the swarm area provides a linkage between an anomalous upper mantle body and the postulated melt transport in the crust. All these processes are observed close to the tip of the northward directing Lake George rift segment, in an area where the Rwenzori Mountains are linked to the rift shoulder. This could indicate that we presently observe the initial rifting stage of a propagating rift segment which may eventually lead to the complete detachment of the Rwenzoris from the surrounding rift flanks in the future as proposed by Koehn et al. (2008) by numerical modelling. In such an early rifting stage it is conceivable that migrating fluids within the crust develop before tectonic evidence is visible at the surface. However, the observation of fluid induced swarm activity alone is certainly not a sufficient proof for this conceptual model. Additional evidence has to come from other disciplines.

Acknowledgements

This study has been funded by the Deutsche Forschungsgemeinschaft (DFG) in the framework of the RiftLink research group (www.riftlink.org). We appreciate the support of the Ugandan National Council for

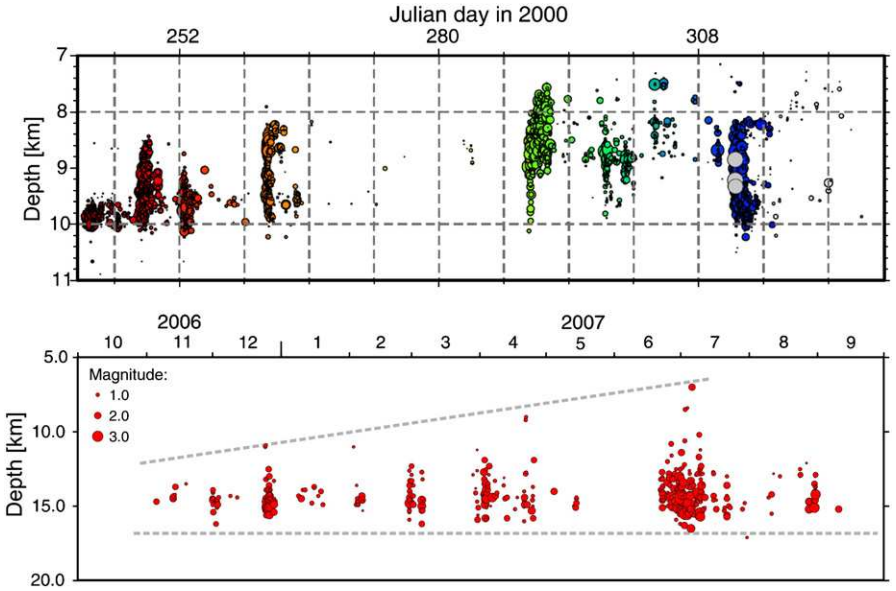

Fig. 12. Comparison of the spatio-temporal properties of two earthquake swarms. Top: Eger rift (from Dahm et al., 2008, Fig. 6). Bottom: Rwenzori, cluster 2 (cf. Fig. 3). The two earthquake clusters show similar characteristics of their individual swarm components, such as duration of activity, vertical extent, migration tendencies, and magnitude distribution.

Science and Technology (UNCST), the Ugandan Wildlife Authority (UWA), and the Geology Department of the Makerere University in Kampala. We thank Andreas Schumann for coordination of the field work. We also thank the Geophysical Instrumentation Pool Potsdam (GIPP) for providing the seismological equipment and GEOFON for archiving the data. Data processing and visualization was done with SEISAN and GMT software.

Appendix A. Supplementary data

Supplementary data to this article can be found online at http://dx.doi.org/10.1016/j.tecto.2012.07.010.

References

Albaric, J., Déverchère, J., Petit, C., Perrot, J., Le Gall, B., 2009. Crustal rheology and depth distribution of earthquakes: Insights from the central and southern East African Rift System. Tectonophysics 468, 28–41.

Albaric, J., Perrot, J., Déverchère, J., Deschamps, A., Le Gall, B., Ferdinand, R.W., Petit, C., Tiberi, C., Sue, C., Songo, M., 2010. Contrasted seismogenic and rheological behaviours from shallow and deep earthquake sequences in the North Tanzanian Divergence, East Africa. Journal of African Earth Sciences 58, 799–811. http://dx.doi.org/10.1016/j.jafrearsci.2009.09.005.

Arad, A., Morton, W.H., 1969. Mineral springs and saline lakes of Western Rift Valley, Uganda. Geochimica et Cosmochimica Acta 33, 1169–1181.

Baer, G., Hamiel, Y., Shamir, G., Nof, R., 2008. Evolution of a magma-driven earthquake swarm and triggering of the nearby Oldoinyo Lengai eruption, as resolved by InSAR, ground observations and elastic modeling, East African Rift, 2007. Earth and Planetary Science Letters 272, 339–352. http://dx.doi.org/10.1016/j.epsl.2008.04.052.

Bahati, G., Pang, Z.H., Armannsson, H., Isabirye, E.M., Kato, V., 2005. Hydrology and reservoir characteristics of three geothermal systems in western Uganda. Geothermics 34, 568–591.

Bailey, K., et al., 2005. Melilitite at Fort Portal, Uganda: another dimension to the carbonate volcanism. Lithos 85, 15–25.

Barker, D.S., Nixon, P.H., 1989. High-Ca, low-alkali carbonatite volcanism at Fort Portal, Uganda. Contributions to Mineralogy and Petrology 103, 166–177.

Battaglia, J., Ferrazzini, V., Staudacher, T., Aki, K., 2005. Pre-eruptive migration of earthquakes at the Piton de la Fournaise volcano (Réunion Island). Geophysical Journal International 161, 549–558.

Benoit, J.P., McNutt, S.R., 1996. Global volcanic earthquake swarm database 1979–1989. Open-file Report, vol. 69. U. S. Geological Survey. 31 pp.

Boven, A., Pasteels, P., Punzalan, L.E., Yamba, T.K., Musisi, J.H., 1998. Quaternary perpotassic magmatism in Uganda (Tore-Ankole Volcanic Province): age assessment and significance for magmatic evolution along the East African Rift. Journal of African Earth Sciences 26, 463–476.

Bräuer, K., Kämpf, H., Strauch, G., Weise, S.M., 2003. Isotopic evidence ($^3He/^4He$, $^{13}C_{CO2}$) of fluid-triggered intraplate seismicity. Journal of Geophysical Research 108 (B2), 2070. http://dx.doi.org/10.1029/2002JB002077.

Bridges, D.L., Gao, S., 2006. Spatial variation of seismic b-values beneath Makushin Volcano, Unalaska Island, Alaska. Earth and Planetary Science Letters 245, 408–415. http://dx.doi.org/10.1016/j.epsl.2006.03.010.

Brooker, R.A., Kjarsgaard, B.A., 2011. Silicate-carbonate liquid immiscibility and phase relations in the system SiO_2-Na_2O_3-CaO-CO_2 at 0.1–2.5 GPa with applications to carbonatite genesis. Journal of Petrology 52, 1281–1305.

Brooker, R.A., Kohn, S.C., Holloway, J.R., McMillan, P.F., 2001. Structural controls on the solubility of CO_2 in silicate melts Part I: bulk solubility data. Chemical Geology 174, 225–239.

Brooks, A.S., Smith, C.C., 1987. Ishango revisited: new age determinations and cultural interpretations. African Archaeological Review 5, 65–78.

Crampin, S., Chastin, S., 2003. A review of shear wave splitting in the crack-critical crust. Geophysical Journal International 155, 221–240.

Dahm, T., Fischer, T., Hainzl, S., 2008. Mechanical intrusion models and their implications for the possibility of magma-driven swarms in NW Bohemia region. Studia Geophysica et Geodaetica 52, 529–548.

Dixon, J.E., 1997. Degassing of alkalic basalts. American Mineralogist 82, 368–378.

Dixon, C.G., Morton, W.H., 1970. Thermal and mineral springs in Uganda. Geothermics 2, 1035–1038.

Ebinger, C.J., Keir, D., Ayele, A., Calais, E., Wright, T.J., Belachew, M., Hammond, J.O.S., Campbell, E., Buck, W.R., 2008. Capturing magma intrusion and faulting processes during continental rupture: seismicity of the Dabbahu (Afar) rift. Geophysical Journal International 174, 1138–1152. http://dx.doi.org/10.1111/j.1365-246X.2008.03877.x.

Eggler, D.H., 1989. Carbonatites, primary mantle melts and mantle dynamics. Carbonatites: Genesis and Evolution. Unwin Hyman, London, pp. 580–600.

Fairhead, J.D., Girdler, R.W., 1971. The seismicity of Africa. Journal of the Royal Astronomical Society 24, 271–301.

Foley, S.F., Link, K., Tiberindwa, J.V., Barifaijo, E., 2012. Patterns and origin of igneous activity around the Tanzanian craton. Journal of African Earth Sciences 62, 1–18.

Foster, A., Jackson, J.A., 1998. Source parameters of large African earthquakes: implications for crustal rheology and regional kinematics. Geophysical Journal International 134, 422–448.

Gardine, M., West, M., Werner, C., Doukas, M., 2011. Evidence of magma intrusion at Fourpeaked Volcano, Alaska in 2006–2007 from a rapid-response seismic network and volcanic gases. Journal of Volcanology and Geothermal Research 200, 192–200. http://dx.doi.org/10.1016/j.jvolgeores.2010.11.018.

Geissler, W.H., Kämpf, H., Kind, R., Bräuer, K., Klinge, K., Plenefisch, T., Horálek, J., Zedník, J., Nehybka, V., 2005. Seismic structure and location of a CO_2 source in the upper mantle of the western Eger (Ohře) rift, central Europe. Tectonics 24, TC5001. http://dx.doi.org/10.1029/2004TC001672.

Grünthal, G., 1989. About the history of earthquake activity in the focal region Vogtland/Western Bohemia. In: Bormann, P. (Ed.), Monitoring and Analysis of the Earthquake Swarm 1985/86 in the Region Vogtland/Western Bohemia. Akad. der Wissensch. der DDR, Potsdam, pp. 30–34.

Hainzl, S., 2004. Seismicity patterns of earthquake swarms due to fluid intrusion and stress triggering. Geophysical Journal International 159, 1090–1096. http://dx.doi.org/10.1111/j.1365-246X.2004.02463.x.

Hainzl, S., Ogata, Y., 2005. Detecting fluid signals in seismicity data through statistical earthquake modelling. Journal of Geophysical Research 110, B05S07. http://dx.doi.org/10.1029/2004JB003247.

Hayashi, Y., Morita, Y., 2003. An image of a magma intrusion process inferred from precise hypocentral migrations of the earthquake swarm east of the Izu Peninsula. Geophysical Journal International 153, 159–174.

Hensch, M., Riedel, C., Reinhardt, J., Dahm, T., the NICE-People, 2008. Hypocenter migration of fluid-induced earthquake swarms in the Tjörnes Fracture Zone. Tectonophysics 447, 80–94. http://dx.doi.org/10.1016/j.tecto.2006.07.015.

Hogarth, D.D., Horne, J.E., 1989. Non-metamict uranoan pyrochlore and uranpyrochlore from tuff near Ndale, Fort Portal area, Uganda. Mineralogical Magazine 53, 257–262.

Ibs-von Seht, M., Blumenstein, S., Wagner, R., Hollnack, D., Wohlenberg, J., 2001. Seismicity, seismotectonics and crustal structure of the southern Kenya rift—new data from the Lake Magadi Area. Geophysical Journal International 146, 439–453.

Ibs-von Seht, M., Plenefisch, T., Klinge, K., 2008. Earthquake swarms in continental rifts—a comparison of selected cases in America, Africa and Europe. Tectonophysics 452, 66–77.

Jakobsdóttir, S.S., Roberts, M.J., Guđmundsson, G.B., Geirsson, H., Slunga, R., 2008. Earthquake swarms at Upptyppingar, north-east Iceland: a sign of magma intrusion? Studia Geophysica et Geodaetica 52, 513–528.

Karpin, T.L., Thurber, C.H., 1987. The relationship between earthquake swarms and magma transport: Kilauea Volcano, Hawaii. Pure and Applied Geophysics 125, 971–991.

Kato, V., 2000. Geothermal field studies using stable isotope hydrology: case studies in Uganda and Iceland. Geothermal Training programme, report no. 10. The United Nations University, Reykjavik, pp. 189–216.

Keir, D., Pagli, C., Bastow, I.D., Ayele, A., 2011. The magma assisted removal of Arabia in Afar: evidence from dike injection in the Ethiopian rift captured using InSAR and seismicity. Tectonics 30, TC2008. http://dx.doi.org/10.1029/2010TC002785.

Key, J., White, R.S., Soosalu, H.E., Jakobsdóttir, S.S., 2011. Multiple melt injection along a spreading segment at Askja, Iceland. Geophysical Research Letters 38, L05301. http://dx.doi.org/10.1029/2010GL046264.

Koehn, D., Aanyu, K., Haines, S., Sachau, T., 2008. Rift nucleation, rift propagation and the creation of basement micro-plates within active rifts. Tectonophysics 458, 105–116.

Koehn, D., Lindenfeld, M., Rümpker, G., Aanyu, K., Haines, S., Passchier, C.W., Sachau, T., 2010. Active transsection faults in rift transfer zones: evidence for complex stress fields and implications for crustal fragmentation processes in the western branch of the East African Rift. International Journal of Earth Sciences 99, 1633–1642.

Lindenfeld, M., Rümpker, G., 2011. Detection of mantle earthquakes beneath the East African Rift. Geophysical Journal International 186, 1–5. http://dx.doi.org/10.1111/j.1365-246X.2011.05048.x.

Lindenfeld, M., Rümpker, G., Batte, A., Schumann, A., 2012. Seismicity at the Rwenzori Mountains, East African Rift: earthquake distribution, magnitudes and source mechanisms. Solid Earth Discussion 4, 565–598. http://dx.doi.org/10.5194/sed-4-565-2012.

Link, K., et al., 2010. Continuous cratonic crust between the Congo and Tanzania blocks in western Uganda. International Journal of Earth Sciences 99, 1559–1573.

Maasha, N., 1975. The seismicity of the Rwenzori region in Uganda. Journal of Geophysical Research 80, 1485–1496.

Mogi, K., 1963. Some discussions on aftershocks, foreshocks and earthquake swarms—the fracture of a semi-infinite body caused by an inner stress origin and its relation to the earthquake phenomena. Bulletin of the Earthquake Research Institute, University of Tokyo 41, 615–658.

Morley, C.K., 1999. Geoscience of rift systems-evolution of East Africa. AAPG Studies in Geology 44, 242.

Newman, S., Lowenstern, J.B., 2002. VOLATILECALC: a silicate melt-H_2O-CO_2 solution model written in Visual Basic for excel. Computers & Geosciences 28, 597–604.

Nyblade, A.A., Langston, C.A., 1995. East African earthquakes below 20 km depth and their implications for crustal structure. Geophysical Journal International 121, 49–62.

Rosenthal, A., Foley, S.F., Pearson, D.G., Nowell, G.M., Tappe, S., 2009. Petrogenesis of strongly alkaline primitive volcanic rocks at the propagating tip of the western branch of the East African Rift. Earth and Planetary Science Letters 284, 236–248.

Snoke, J.A., Munsey, J.W., Teague, A.C., Bollinger, G.A., 1984. A program for focal mechanism determination by combined use of polarity and SV-P amplitude ratio data. Earthquake Notes 55, 51.

Soosalu, H., Key, J., White, R.S., Knox, C., Einarsson, P., Jakobsdóttir, S.S., 2010. Lower-crustal earthquakes caused by magma movement beneath Askja volcano on the north Iceland rift. Bulletin of Volcanology 72, 55–62. http://dx.doi.org/10.1007/s00445-009-0297-3.

Špičák, A., 2000. Earthquake swarms and accompanying phenomena in intraplate regions: a review. Studia Geophysica et Geodaetica 44, 89–106.
Špičák, A., Horálek, J., 2001. Possible role of fluids in the process of earthquake swarm generation in the West Bohemia/Vogtland seismoactive region. Tectonophysics 336, 151–161.
Špičák, A., Horálek, J., Bouskova, A., Tomek, Č., Vanek, J., 1999. Magma intrusions and earthquake swarm occurrence in the western part of the Bohemian Massif. Studia Geophysica et Geodaetica 43, 87–106.
Stamps, D.S., Calais, E., Saria, E., Hartnady, Ch., Nocquet, J.M., Ebinger, C.J., Fernandes, R.M., 2008. A kinematic model for the East African Rift. Geophysical Research Letters 35, L05304. http://dx.doi.org/10.1029/2007GL032781.
Stamps, D.S., Flesch, L.M., Calais, E., 2010. Lithospheric buoyancy forces in Africa from a thin sheet approach. International Journal of Earth Sciences (Geologische Rundschau) 99, 1525–1533. http://dx.doi.org/10.1007/s00531-010-0533-2.
Stoppa, F., Woolley, A.R., Lloyd, F.E., Eby, N.G., 2000. Carbonatite lapilli-bearing tuff and a dolomite carbonatite bomb form Murumuli crater, Katwe volcanic field, Uganda. Mineralogical Magazine 64, 641–650.
Tarasewicz, J., Brandsdóttir, B., White, R.S., Hensch, M., Thorbjarnardóttir, B., 2012. Using microearthquakes to track repeated magma intrusions beneath the Eyjafjallajökull stratovolcano, Iceland. Journal of Geophysical Research 117, B00C06. http://dx.doi.org/10.1029/2011JB008751.
Tongue, J.A., Maguire, P.K.H., Burton, P., 1994. An earthquake study in the Lake Baringo basin of the central Kenya rift. Tectonophysics 236, 151–164.
Tugume, F.A., Nyblade, A.A., 2009. The depth distribution of seismicity at the northern end of the Rwenzori mountains: implications for heat flow in the western branch of the East African Rift System in Uganda. South African Journal of Geology 112, 261–271.
Twesigomwe, E.M., 1997. Seismic hazards in Uganda. Journal of African Earth Sciences 24, 183–195.
Waldhauser, F., Ellsworth, W.L., 2000. A double-difference earthquake location algorithm: method and application to the northern Hayward fault, California. Bulletin of the Seismological Society of America 90, 1353–1368.
Weise, S.M., Bräuer, K., Kämpf, H., Strauch, G., Koch, U., 2001. Transport of mantle volatiles through the crust traced by seismically released fluids: a natural experiment in the earthquake swarm area Vogtland/NW Bohemia, Central Europe. Tectonophysics 336, 137–150.
White, R.S., Drew, J., Martens, H.R., Key, J., Soosalu, H., Jakobsdóttir, S.S., 2011. Dynamics of dyke intrusion in the mid-crust of Iceland. Earth and Planetary Science Letters 304, 300–312. http://dx.doi.org/10.1016/j.epsl.2011.02.038.
Wiemer, S., Wyss, M., 2002. Mapping spatial variability of the frequency-magnitude distribution of earthquakes. Advances in Geophysics 45, 259–302.
Wölbern, I., Rümpker, G., Schumann, A., Muwanga, A., 2010. Crustal thinning beneath the Rwenzori region, Albertine rift, Uganda, from receiver-function analysis. International Journal of Earth Sciences (Geologische Rundschau) 99, 1545–1557.
Wölbern, I., Rümpker, G., Link, K., Sodoudi, F., 2012. Melt infiltration of the lower lithosphere beneath the Tanzania craton and the Albertine rift inferred from S receiver functions. Geochem. Geophys. Geosyst. 13, Q0AK08. http://dx.doi.org/10.1029/2012GC004167.
Young, P.A.V., Maguire, P.K.H., Laffoley, N.d'A., Evans, J.R., 1991. Implications of the distribution of seismicity near Lake Bogoria in the Kenya Rift. Geophysical Journal International 105, 665–674.
Zoback, M.D., Harjes, H.-P., 1997. Injection-induced earthquakes and crustal stress at 9 km depth at the KTB deep drilling site, Germany. Journal of Geophysical Research 102, 18477–18491. http://dx.doi.org/10.1029/96JB02814.